Does the Borexino experiment have enough resolution to detect the neutrino flavor day-night asymmetry?

S. S. Aleshin*, O. G. Kharlanov†, A. E. Lobanov‡
Department of Theoretical Physics, Faculty of Physics, Moscow State University, 119991 Moscow, Russia

Abstract

The Earth's density distribution can be approximately considered piecewise continuous at the scale of two-flavor oscillations of neutrinos with energies about 1 MeV. This quite general assumption appears to be enough to analytically calculate the day-night asymmetry factor. Using the explicit time averaging procedure, we show that, within the leading-order approximation, this factor is determined by the electron density immediately before the detector, i.e. in the Earth's crust. Within the approximation chosen, the resulting asymmetry factor does not depend either on the properties of the inner Earth's layers or on the substance and the dimensions of the detector. For beryllium neutrinos, we arrive at the asymmetry factor estimation of about -3.8×10^{-4}, which is at least one order of magnitude beyond the present experimental resolution, including that of the Borexino experiment.

1 Introduction

The effect of neutrino oscillations in vacuum lies beyond the Standard Model and is thus interesting both from the theoretical and experimental point of view. The oscillations in medium are also studied since Wolfenstein, who showed that the neutrinos acquire a specific flavor-dependent potential due to the coherent forward scattering on the matter [1]. As a result, the neutrino propagation in medium should demonstrate the conversion from one flavor into another (i.e. flavor oscillations), even if the vacuum mixing is negligible. This spectacular result is known as the Mikheev–Smirnov–Wolfenstein effect [2] and suffices to explain the deficit of observed solar electron neutrinos [3]. According to Mikheev and Smirnov, the leading-order estimation for the electron neutrino flux depends only on the points where the neutrino was born (the core of the Sun) and absorbed (the detector). However, the properties of the medium between these two points can also slightly affect the flavor composition of the observed neutrino flux, leading, in particular, to the day-night (solar neutrino flavor) asymmetry [4, 5]. The latter effect being crucial for the entire flavor oscillations framework, a number of experiments were set up to catch this slight flavor composition variation resulting from the nighttime neutrino propagation through the Earth. In April 2011, the Borexino collaboration did report the possible observation of the asymmetry at the level of 10^{-3} for beryllium neutrinos, however, with a high uncertainty [6]. Since other neutrino experiments have already yielded a considerable amount of data on the vacuum neutrino mixing [7, 8], the question is whether it is really worth looking forward to the experimental discovery of the day-night asymmetry in the nearest future. Namely, one may ask: based on the data provided by other experiments, how close is

*e-mail: aless2001@mail.ru
†e-mail: okharl@mail.ru
‡e-mail: lobanov@phys.msu.ru

the theoretically predicted asymmetry to the present experimental resolution? According to the analysis presented below, the magnitude of the day-night asymmetry is separated from this resolution by at least one order of magnitude.

Within the neutrino oscillations framework, it is common to use the Schroedinger-like equation to describe the spatial variations of the neutrino flavor [1, 2]. Within the two-flavor approximation, the Schroedinger problem is posed in terms of the 2×2 flavor evolution matrix (operator) $R(x, x_0)$, whose elements are the neutrino flavor transition amplitudes after traveling from the point x_0 to x. The evolution equation and the initial condition read, respectively,

$$\frac{\partial R(x, x_0)}{\partial x} = -\mathrm{i}\lambda A(x) R(x, x_0), \tag{1}$$

$$R(x_0, x_0) = \mathbb{1}, \tag{2}$$

where the matrix Hamiltonian is a point-dependent linear combination of the Pauli matrices,

$$A(x) = a(x)\sigma_3 + b\sigma_1, \tag{3}$$

$$a(x) = -\cos 2\theta_0 + \frac{2EV(x)}{\Delta m^2}, \qquad b = \sin 2\theta_0. \tag{4}$$

Here, θ_0 is the vacuum mixing angle, E is the neutrino energy, Δm^2 is the difference between squared neutrino masses, and $V(x) = \sqrt{2} G_\mathrm{F} N_e(x)$ is the Wolfenstein potential, which is proportional to the electron density in the medium N_e and the Fermi constant G_F. The constant coefficient $\lambda = \Delta m^2 / 4E$ is the reciprocal neutrino oscillation length, up to the factor of π,

$$\ell_\mathrm{osc} = \frac{4\pi E}{\Delta m^2} = \frac{\pi}{\lambda}. \tag{5}$$

Equation (1) defines a one-parametric subgroup of $SU(2)$ and hence of $SO(3)$, the translation along x being the group operation. In this sense, equation (1) is analogous to the Bargmann–Michel–Telegdi equation [9] in the spinor representation [10]. It is well known that the solution of the matrix linear ordinary differential equation, such as (1), can be represented as a time-ordered exponent (Dyson expansion) [11]. However, in the case of general $N_e(x)$ profile, the solution in terms of a number-valued series without a symbolic operation such as time ordering appears to be too challenging to find. In the recent investigations, considerable progress was made in finding exact solutions of Eq. (1) in certain special cases [12, 13]; nevertheless, the general approach to this kind of equation still remains to be approximate.

Quite a large number of publications are devoted to the analysis of these approximate solutions. Probably the most effective technique for finding the approximate solutions of matrix linear differential equations, such as (1), is the so called Magnus expansion [14], which is a modification of the Baker–Campbell–Hausdorff formula [15]. This approach provides the solution up to any order of approximation, as well as the constraints on the remainder terms [16]. Unfortunately, this technique [17–20], as well as other general methods (see, e.g., [21, 22]), do not provide the way to find the solution in its explicit form, not firmly fixing the Earth model, namely, $N_e(x)$ density distribution. It is thus desirable to find an approximate analytical solution of equation (1), which is valid under quite general assumptions about the electron density profile $N_e(x)$. This idea was developed in [23–25].

In our paper, we are not only aiming at finding the relevant approximate expressions, but also at estimating their accuracy and applicability domain. Namely, in section 2, we find the approximate solutions for the flavor evolution matrix inside the Earth, and then, in section 3, we arrive at the observation probabilities for the neutrinos of different flavors. These probabilities are finally subjected to the averaging procedure due to the continuous observation of the solar neutrinos throughout the year (Sec. 3.2), and the results of this averaging are discussed in section 4. The magnitude of the day-night asymmetry appears to be sensitive to the non-trivial

structure of the Earth's crust under the neutrino detector, so the effect of the crust is paid special attention in section 3.3. In particular, we show that our estimation for the neutrino day-night asymmetry is valid for beryllium neutrinos, which are observed in the Borexino experiment.

2 The Density Profile and the Evolution Matrix

In our investigation, we use the model electron density profile $N_e(x)$ with $n-1$ narrow segments, where it changes steeply, separated by n wide though sloping segments. Let us call these segments cliffs and valleys, respectively. Let the cliffs be localized near points x_j, $j = \overline{1, n-1}$, namely, occupy the segments $[x_j^-, x_j^+]$ of widths ϵ_j, where $x_j^\pm \equiv x_j \pm \epsilon_j/2$. Then the valleys are $[x_{j-1}^+, x_j^-]$ and have the widths $L_j \approx x_j - x_{j-1}$. In fact, this kind of model is a good approximation for the Earth's density profile known in geophysics, where it corresponds to the so-called Preliminary Reference Earth Model (PREM) [26,27]. Inside the Earth, the oscillation lengths of neutrinos with $E \sim 1$MeV are of the order of 30km, and the inequality

$$\epsilon_j \ll \ell_{\rm osc} \ll L_j \tag{6}$$

takes place, i.e. the cliffs are narrow and the valleys are wide compared with the oscillation length. In the following, we will briefly call such density distribution piecewise continuous. It is worth saying here that during the night, the neutrino ray traverses different paths through the Earth, thus, the lengths ϵ_j and L_j vary. However, the assumption (6) holds for the most part of the night.

The total flavor evolution operator for such piecewise continuous density profile equals the matrix product of the evolution operators for all cliffs and valleys. Within each of these segments, the two small parameters arise: the first of them,

$$\eta = \frac{2EV(x)}{\Delta m^2} \lesssim 10^{-2} \qquad (E \sim 1 \text{ MeV}) \tag{7}$$

due to the relatively small density of the Earth [24,28], while the second parameter due to the piecewise continuous structure of the density profile,

$$\delta = \begin{cases} \ell_{\rm osc}/L_j & \text{for } j\text{th valley,} \\ \epsilon_j/\ell_{\rm osc} & \text{for } j\text{th cliff.} \end{cases} \tag{8}$$

The evolution matrix for each segment, as well as the total evolution matrix, can be subjected to the following unitary transformations [19]:

$$R(x, x_0) = Z^+(x) Y(\psi(x)) R_0(x, x_0) Y^{-1}(\psi(x_0)) Z^-(x_0), \tag{9}$$

$$Z^\pm(x) = \frac{1}{\sqrt{2}} \left\{ \sqrt{1 - \frac{a(x)}{\omega(x)}} \pm {\rm i}\sigma_2 \sqrt{1 + \frac{a(x)}{\omega(x)}} \right\}, \tag{10}$$

$$Y(\psi(x)) = \cos\psi(x) + {\rm i}\sigma_3 \sin\psi(x) = \exp\{{\rm i}\sigma_3 \psi(x)\}, \tag{11}$$

where $\omega(x) = \sqrt{a^2(x) + b^2}$ is the effective oscillation wave number and $\psi(x) = \lambda \int \omega(x) {\rm d}x$ is the corresponding phase incursion. For the calculations which follow, it is also useful to introduce the effective mixing angle in the medium $\theta(x)$ [2], which is defined by the expressions

$$\cos 2\theta(x) = -\frac{a(x)}{\omega(x)}, \qquad \sin 2\theta(x) = \frac{b}{\omega(x)}. \tag{12}$$

In terms of this angle,

$$Z^\pm(x) = \exp\{\pm {\rm i}\sigma_2 \theta(x)\}. \tag{13}$$

The transformation with matrices $Z^{\pm}(x)$ locally diagonalizes the Hamiltonian $A(x)$ in the point x. It thus makes the complete diagonalization in the homogeneous case $N_e(x) = \text{const}$ [2]. The transformation with the operator $Y(\psi(x))$ isolates the effect of the medium inhomogeneity, the transformed evolution matrix $R_0(x, x_0)$ satisfying the equation

$$\frac{\partial R_0(x, x_0)}{\partial x} = -\mathrm{i}\dot{\theta}(x)\sigma_2 e^{2\mathrm{i}\sigma_3\psi(x)} R_0(x, x_0), \tag{14}$$

where the dot over θ denotes the gradient

$$\dot{\theta}(x) \equiv \partial_x \theta(x) = \frac{b\,\partial_x a(x)}{2\omega^2(x)}. \tag{15}$$

Due to the fact that the neutrino detector is homogeneous ($\dot{\theta}(x) = 0$), Eq. (14) has a well-defined and physically relevant $x \to +\infty$ limit for any fixed x_0. Moreover, asymptotically convergent behavior of such systems of differential equations is stated by the Levinson theorem [11].

In the homogeneous case, the equation above is trivial, $R_0(x, x_0) \equiv \mathbb{1}$. However, in the valley $[x_j^+, x_{j+1}^-]$, the slow change of the density $N_e(x)$ enables us to use the so-called adiabatic approximation leading to the same result [2]

$$R_0(x_{j+1}^-, x_j^+) = \mathbb{1} + O(\eta\delta_{\text{valley}}), \tag{16}$$

where the remainder term is a (generally speaking, non-diagonal) matrix. On the other hand, if the Wolfenstein potential undergoes a considerable change within the narrow cliff $[x_j^-, x_j^+]$ with the phase incursion $\Delta\psi \ll 2\pi$, then we get

$$R_0(x_j^+, x_j^-) = \exp\left\{-\mathrm{i}\sigma_2\Delta\theta_j e^{2\mathrm{i}\sigma_3\psi(x_j^-)}\right\} + O(\eta\delta_{\text{cliff}}), \tag{17}$$

where $\Delta\theta_j \equiv \theta(x_j^+) - \theta(x_j^-) = O(\eta)$ is the jump of the effective mixing angle on the jth cliff. Moreover, one can show that within the more accurate $O(\eta\delta)$ approximation, the above expressions take the form

$$R_0(x_{j+1}^-, x_j^+) = \exp\left\{-\frac{\mathrm{i}\sigma_1}{2\lambda}\left[e^{2\mathrm{i}\sigma_3\psi(x_{j+1}^-)}\dot{\theta}(x_{j+1}^-) - e^{2\mathrm{i}\sigma_3\psi(x_j^+)}\dot{\theta}(x_j^+)\right]\right\} + O(\eta\delta^2)(\text{valley}), \tag{18}$$

$$R_0(x_j^+, x_j^-) = \exp\{(-\mathrm{i}\sigma_2\Delta\theta_j + \mathrm{i}\sigma_1\mu_j)e^{2\mathrm{i}\sigma_3\psi(x_j^-)}\} + O(\eta\delta^2) \qquad (\text{cliff}), \tag{19}$$

where

$$\mu_j = 2\lambda\int_{x_j^-}^{x_j^+}(y - x_j^-)\dot{\theta}(y)\mathrm{d}y = O(\eta\delta). \tag{20}$$

Now let us write the evolution operator for the whole neutrino path. The neutrinos observed during the day are created in the point x_0 inside the solar core, then travel to the Earth, enter the detector in the point x_1 and are finally absorbed in the point x^* inside it. In the nighttime, however, after reaching the Earth in the point x_1, the neutrinos pass through $n-1$ Earth's layers (valleys) discussed above, and only after that they enter the detector in the point x_n and are absorbed in x^*. Crossing the Sun-to-vacuum interface, as well as traveling inside the Sun, does not involve steep electron density changes, thus we can treat the whole segment $[x_0, x_1]$ as a single valley. As it was mentioned earlier, the flavor evolution operator for the whole neutrino path is a matrix product of the evolution operators for each segment (each valley and cliff). By the substitution of the approximate solutions (18) and (19) into representation (9), after some transformations we find the total evolution operator in the form

$$\begin{aligned} R(x^*, x_0) &= R_{\text{det}}(x^*, x_n^+)e^{\mathrm{i}\sigma_2\theta_n^-}e^{\mathrm{i}\sigma_1(\mu_n - \dot{\theta}_n^-/2\lambda)}e^{\mathrm{i}\sigma_3\Delta\psi_n}e^{-\mathrm{i}\sigma_2\Delta\theta_{n-1}}e^{\mathrm{i}\sigma_1\bar{\mu}_{n-1}} \\ &\times\ e^{\mathrm{i}\sigma_3\Delta\psi_{n-1}}e^{-\mathrm{i}\sigma_2\Delta\theta_{n-2}}e^{\mathrm{i}\sigma_1\bar{\mu}_{n-2}}e^{\mathrm{i}\sigma_3\Delta\psi_{n-2}}\ldots \\ &\times\ e^{\mathrm{i}\sigma_3\Delta\psi_2}e^{-\mathrm{i}\sigma_2\Delta\theta_1}e^{\mathrm{i}\sigma_1\bar{\mu}_1}e^{\mathrm{i}\sigma_3\Delta\psi_1}e^{\mathrm{i}\sigma_1\dot{\theta}_{\text{Sun}}/2\lambda}e^{-\mathrm{i}\sigma_2\theta_{\text{Sun}}} + O(n\eta\delta^2). \end{aligned} \tag{21}$$

Here, the subscript 'Sun' refers to the point x_0 inside the solar core, where the neutrino is created, and the evolution operator inside the neutrino detector is denoted $R_{\rm det}$. The factor n in the remainder term indicates that it contains the sum over all cliffs and valleys. Moreover, we use the following notation:

$$\theta_j^- \equiv \theta(x_j^-), \quad \Delta\theta_j \equiv \theta(x_j^+) - \theta(x_j^-), \qquad j = \overline{1, n-1}, \tag{22}$$

$$\dot\theta_j^- \equiv \dot\theta(x_j^-), \quad \Delta\dot\theta_j \equiv \dot\theta(x_j^+) - \dot\theta(x_j^-), \qquad j = \overline{1, n-1}, \tag{23}$$

$$\bar\mu_j \equiv \mu_j + \frac{\Delta\dot\theta_j}{2\lambda} = \int\limits_{x_j^-}^{x_j^+} \left(2\lambda(x - x_j^-)\dot\theta(x) + \frac{\ddot\theta(x)}{2\lambda} \right) {\rm d}x, \qquad j = \overline{1, n-1}, \tag{24}$$

$$\Delta\psi_j \equiv \psi(x_j^-) - \psi(x_{j-1}^-) = \lambda \int\limits_{x_{j-1}^-}^{x_j^-} \omega(x){\rm d}x, \qquad j = \overline{1, n}. \tag{25}$$

It is also convenient to append definition (24) with

$$\bar\mu_n \equiv \mu_n - \dot\theta_n^-/2\lambda, \quad \bar\mu_0 \equiv \dot\theta_{\rm Sun}/2\lambda. \tag{26}$$

If the boundary between the Earth's crust and the detector is abrupt, $x_n^+ - x_n^- \ll \ell_{\rm osc}$, then μ_n vanishes. Quite analogously, μ_1 vanishes for the abrupt vacuum-to-Earth boundary.

By projecting the neutrino state onto the flavor eigenstates, we arrive at the observation probabilities for the electron/muon neutrino

$$P_{e,\mu} \equiv \left\{ \begin{array}{c} P(\nu_e \to \nu_e) \\ P(\nu_e \to \nu_\mu) \end{array} \right\} = \frac{1}{2} \pm \frac{1}{4} {\rm Sp}\left\{ R(x^*, x_0)\sigma_3 R^\dagger(x^*, x_0)\sigma_3 \right\} = \frac{1 \pm T}{2}, \tag{27}$$

where, for nighttime neutrinos,

$$\begin{aligned} T_{\rm night} &= \frac{1}{2}{\rm Sp}\big\{ \sigma_3 R_{\rm det}^\dagger(x^*, x_n^+)\sigma_3 R_{\rm det}(x^*, x_n^+) e^{{\rm i}\sigma_2\theta_n^-} e^{{\rm i}\sigma_1\bar\mu_n} e^{{\rm i}\sigma_3\Delta\psi_n} e^{-{\rm i}\sigma_2\Delta\theta_{n-1}} e^{{\rm i}\sigma_1\bar\mu_{n-1}} e^{{\rm i}\sigma_3\Delta\psi_{n-1}} \\ &\times\ e^{-{\rm i}\sigma_2\Delta\theta_{n-2}} e^{{\rm i}\sigma_1\bar\mu_{n-2}} e^{{\rm i}\sigma_3\Delta\psi_{n-2}} \ldots e^{-{\rm i}\sigma_2\Delta\theta_1} e^{{\rm i}\sigma_1\bar\mu_1} e^{{\rm i}\sigma_3\Delta\psi_1} e^{{\rm i}\sigma_1\bar\mu_0} e^{-2{\rm i}\sigma_2\theta_{\rm Sun}} \\ &\times\ e^{{\rm i}\sigma_1\bar\mu_0} e^{-{\rm i}\sigma_3\Delta\psi_1} e^{{\rm i}\sigma_1\bar\mu_1} e^{-{\rm i}\sigma_2\Delta\theta_1} \ldots e^{-{\rm i}\sigma_3\Delta\psi_{n-1}} e^{{\rm i}\sigma_1\bar\mu_{n-1}} e^{-{\rm i}\sigma_2\Delta\theta_{n-1}} e^{{\rm i}\sigma_1\bar\mu_n} e^{-{\rm i}\sigma_3\Delta\psi_n} e^{{\rm i}\sigma_2\theta_n^-} \big\}, \end{aligned} \tag{28}$$

while for daytime neutrinos we have

$$T_{\rm day} = \frac{1}{2}{\rm Sp}\big\{ \sigma_3 R_{\rm det}^\dagger(x^*, x_n^+)\sigma_3 R_{\rm det}(x^*, x_n^+) e^{{\rm i}\sigma_2\theta_0} e^{{\rm i}\sigma_3\Delta\psi_1} e^{{\rm i}\sigma_1\bar\mu_0} e^{-2{\rm i}\sigma_2\theta_{\rm Sun}} e^{{\rm i}\sigma_1\bar\mu_0} e^{-{\rm i}\sigma_3\Delta\psi_1} e^{{\rm i}\sigma_2\theta_0} \big\}. \tag{29}$$

In the latter expression, we have omitted the exponential involving $\bar\mu_1$, considering the abrupt density change on the entry into the Earth. The mixing angle immediately before the detector obviously takes the vacuum value θ_0 in this case. Moreover, the parameter $\bar\mu_0 = \dot\theta_{\rm Sun}/2\lambda$ is proportional to the inverse radius of the solar core and is thus much smaller than the other μ_j parameters.

Due to the homogeneity of the detector substance and its smallness compared with the oscillation length, we easily find

$$R_{\rm det}(x^*, x_n^+) = Z_{\rm det}^+ e^{{\rm i}\sigma_3\Delta\psi_{\rm det}} Z_{\rm det}^- = e^{{\rm i}\sigma_2\theta_{\rm det}}(\mathbb{1} + {\rm i}\sigma_3\Delta\psi_{\rm det}) e^{-{\rm i}\sigma_2\theta_{\rm det}} + O(\delta_{\rm det}^2), \tag{30}$$

$$\sigma_3 R_{\rm det}^\dagger(x^*, x_n^+)\sigma_3 R_{\rm det}(x^*, x_n^+) = \mathbb{1} - 2{\rm i}\sigma_1\Delta\psi_{\rm det}\sin 2\theta_{\rm det} + O(\delta_{\rm det}^2), \tag{31}$$

where the small parameter $\delta_{\rm det}$ is the ratio of the detector width $L_{\rm det}$ to the oscillation length $\ell_{\rm osc}$. The quadratic remainder terms can obviously be neglected.

3 Day-night asymmetry

3.1 Finding the probabilities

In order to evaluate the probabilities obtained above, let us first make the averaging over the phase $\Delta\psi_1$, which corresponds to the neutrino path between the creation point x_0 and the Earth. The region of the neutrino creation is extremely large compared with the oscillation length, thus, after this averaging, $\langle\cos 2\Delta\psi_1\rangle = \langle\sin 2\Delta\psi_1\rangle = 0$ with a high accuracy. Using this fact together with Eq. (31), after averaging (29) we find, up to the terms of the order $O(\bar\mu_0^2) = O(\eta^2\delta^2)$,

$$\langle e^{\mathrm{i}\sigma_3\Delta\psi_1} e^{\mathrm{i}\sigma_1\bar\mu_0} e^{-2\mathrm{i}\sigma_2\theta_{\rm Sun}} e^{\mathrm{i}\sigma_1\bar\mu_0} e^{-\mathrm{i}\sigma_3\Delta\psi_1}\rangle = \cos 2\theta_{\rm Sun}\cos 2\bar\mu_0 \approx \cos 2\theta_{\rm Sun}, \quad (32)$$

$$\langle T_{\rm day}\rangle = \cos 2\theta_0 \cos 2\theta_{\rm Sun}. \quad (33)$$

The latter expression coincides with the famous result of Mikheev and Smirnov [2]. On the other hand, after averaging over $\Delta\psi_1$ and neglecting $O(\eta^2\delta^2)$ terms, for the nighttime neutrinos we obtain

$$T_{\rm night} \to \frac{1}{2}\cos 2\theta_{\rm Sun}\,\mathrm{Sp}\big\{(e^{2\mathrm{i}\sigma_2\theta_n^-} - 2\mathrm{i}\sigma_1\Delta\psi_{\rm det}\sin 2\theta_{\rm det}) e^{\mathrm{i}\sigma_1\bar\mu_n} e^{\mathrm{i}\sigma_3\Delta\psi_n} e^{-\mathrm{i}\sigma_2\Delta\theta_{n-1}} e^{\mathrm{i}\sigma_1\bar\mu_{n-1}}\ldots$$
$$\times e^{\mathrm{i}\sigma_3\Delta\psi_2} e^{-2\mathrm{i}\sigma_2\Delta\theta_1} e^{2\mathrm{i}\sigma_1\bar\mu_1} e^{-\mathrm{i}\sigma_3\Delta\psi_2}\ldots e^{-\mathrm{i}\sigma_3\Delta\psi_{n-1}} e^{-\mathrm{i}\sigma_2\Delta\theta_{n-1}} e^{\mathrm{i}\sigma_1\bar\mu_{n-1}} e^{-\mathrm{i}\sigma_3\Delta\psi_n} e^{\mathrm{i}\sigma_1\bar\mu_n}\big\}, \quad (34)$$

where we have made use of the fact that matrices $e^{\mathrm{i}\sigma_1\bar\mu_1}$ and $e^{-\mathrm{i}\sigma_2\Delta\theta_1}$ commute up to a negligible term of the order $O(\Delta\theta_1\bar\mu_1)$.

For the calculations which follow, we will use the smallness of the jumps $\Delta\theta_1,\ldots,\Delta\theta_{n-1} = O(\eta)$ and the parameters $\bar\mu_1,\ldots,\bar\mu_n = O(\eta\delta)$. Within the linear approximation in the Earth's density parameter η, this leads to

$$T_{\rm night}(\Delta\theta_1,\ldots,\Delta\theta_{n-1};\bar\mu_1,\ldots,\bar\mu_n) = \cos 2\theta_n^-\cos 2\theta_{\rm Sun}$$
$$+\sum_{j=1}^{n-1}\Delta\theta_j\cdot\left.\frac{\partial T_{\rm night}}{\partial(\Delta\theta_j)}\right|_{\Delta\theta,\bar\mu=0} + \sum_{j=1}^{n}\bar\mu_j\cdot\left.\frac{\partial T_{\rm night}}{\partial\bar\mu_j}\right|_{\Delta\theta,\bar\mu=0}. \quad (35)$$

Partial derivatives with respect to the small parameters are

$$\left.\frac{\partial T_{\rm night}}{\partial(\Delta\theta_j)}\right|_{\Delta\theta,\bar\mu=0} = -\mathrm{i}\cos 2\theta_{\rm Sun}\,\mathrm{Sp}\{(\sigma_2 e^{2\mathrm{i}\sigma_2\theta_n^-} + 2\sigma_3\Delta\psi_{\rm det}\sin 2\theta_{\rm det}) e^{-2\mathrm{i}\sigma_3\Delta\psi_{n,j}}\}$$
$$= 2\cos 2\theta_{\rm Sun}\left\{\sin 2\theta_n^-\cos 2\Delta\psi_{n,j} - 2\Delta\psi_{\rm det}\sin 2\theta_{\rm det}\sin 2\Delta\psi_{n,j}\right\}, \quad (36)$$

$$\left.\frac{\partial T_{\rm night}}{\partial\bar\mu_j}\right|_{\Delta\theta,\bar\mu=0} = \cos 2\theta_{\rm Sun}\,\mathrm{Sp}\{(\mathrm{i}e^{2\mathrm{i}\sigma_2\theta_n^-}\sigma_1 + 2\Delta\psi_{\rm det}\sin 2\theta_{\rm det}) e^{-2\mathrm{i}\sigma_3\Delta\psi_{n,j}}\}$$
$$= 2\cos 2\theta_{\rm Sun}\left\{\sin 2\theta_n^-\sin 2\Delta\psi_{n,j} + 2\Delta\psi_{\rm det}\sin 2\theta_{\rm det}\cos 2\Delta\psi_{n,j}\right\}. \quad (37)$$

In the above expressions,

$$\Delta\psi_{n,j} \equiv \psi(x_n^-) - \psi(x_j^-) = \lambda\int_{x_j^-}^{x_n^-}\omega(x)\mathrm{d}x = \lambda L_{n,j}(1+O(\eta)), \quad (38)$$

where $L_{n,j} \equiv x_n^- - x_j^-$ is the distance between the boundary of the jth shell and the detector, measured along the neutrino ray. Finally, by substituting the derivatives (36) and (37) into Eq. (35) and using the fact that $\sin 2\Delta\psi_{n,n} = 0$, we arrive at the final result

$$T_{\rm night} = \cos 2\theta_{\rm Sun}\Big\{\cos 2\theta_n^- + 2\sin 2\theta_n^-\sum_{j=1}^{n-1}(\Delta\theta_j\cos 2\Delta\psi_{n,j} + \bar\mu_j\sin 2\Delta\psi_{n,j})$$
$$-4\Delta\psi_{\rm det}\sin 2\theta_{\rm det}\sum_{j=1}^{n-1}\Delta\theta_j\sin 2\Delta\psi_{n,j}\Big\}, \quad (39)$$

which is valid up to the terms of the order $O(\eta\delta^2)$ and quadratic terms $O(\eta^2)$. The term involving the product of the detector width $\Delta\psi_{\rm det}$ and the oscillating factor $\bar{\mu}_j \cos 2\Delta\psi_{n,j}$ is of the order $O(\eta\delta\delta_{\rm det})$ and is thus omitted.

The above expression provides a generalization of the main result of paper [25] for the case of nonzero-thickness cliffs and detector. It should be stressed, however, that Eq. (39) gives poor information on the effects to be measured. Indeed, the neutrino experiments last for years, and thus, Eq. (39) may only acquire a predictive power after some kind of averaging. The averaging procedure should take into account the axial rotation of the Earth (involving the integration over the nights), as well as its orbital motion around the Sun.

3.2 Averaging the probabilities

The averaging procedure can be performed analytically, if the oscillation phase incursions $\Delta\psi_{n,j}$ vary by much more than 2π during the night. Namely, in this case, one can employ the stationary phase technique (see, e.g., [29]). In the case of the beryllium neutrinos ($E = 0.862$ MeV) traveling through the Earth, the oscillation length is about 30km, while the widths of the valleys $L_{n,j}$ vary by many hundreds of kilometers, so the oscillation phase variations are indeed large enough to use the stationary phase approximation. The only layer, to which this approximation may not apply, is the Earth's crust immediately under the detector. This layer is discussed in detail in section 3.3 and does not interfere with the picture described in this paragraph.

Let us consider a neutrino traveling through the Earth, which, according to the PREM model [26], consists of a number of concentric spherical shells. The boundary between the valleys x_j corresponds to the point where the neutrino crosses one of the interfaces between the Earth's shells; let r_j be the radius of this interface (see Fig. 1). Further, the distances $L^{\pm}_{n,j}$ between the detector and the points where the neutrino enters/leaves the interface with radius r_j are functions of the 'nadir angle' $\Theta_{\rm N} \in [0, \pi]$ defined as the angle between the direction to the Sun and the nadir in the point of the detector. In terms of the solar elevation angle $\Theta_{\rm s}$ [30], the nadir angle is $\Theta_{\rm N} = \Theta_{\rm s} + \pi/2$. The nadir angle, in turn, is a function of the Earth's axial rotation angle $\tau \in [0, 2\pi)$ ('time of day') and the orbital motion angle $\varsigma \in [0, 2\pi)$ ('season'). The dependence of the distances on the nadir angle is easily found to be

$$L_{n,j} = L^{\pm}_{n,j}(\Theta_{\rm N}) = r_n \cos\Theta_{\rm N} \pm \sqrt{r_j^2 - r_n^2 \sin^2\Theta_{\rm N}}, \tag{40}$$

$$\Theta_{\rm N} \leq \arcsin r_j/r_n, \tag{41}$$

where the upper/lower signs in (40) correspond to the neutrino entering/leaving the interface r_j (see Fig. 1). The inequality (41) ensures that the intersection of the neutrino ray with this interface exists.

In order to find the night average of the electron/muon neutrino observation probabilities, let us note some properties of expressions (39) and (40). First, the number of interfaces crossed by the neutrino is defined via the inequality (41), so the number of the valleys and, thus, the number of terms entering the sums in (39) are changing during the night. The night average of Eq. (39) is therefore the sum of the averages of the terms entering this equation and involving each of the interfaces j, each average being defined as follows:

$$\langle F(\Theta_{\rm N}) e^{2{\rm i}\Delta\psi_{n,j}} \rangle_{\rm night} = \int\limits_{\Theta_{\rm N}(\tau) \leq \arcsin r_j/r_n} F(\Theta_{\rm N}(\tau)) e^{2{\rm i}\Delta\psi_{n,j}(\Theta_{\rm N}(\tau))} \, \frac{{\rm d}\tau}{\Delta\tau_{\rm night}}. \tag{42}$$

Here, $F(\Theta_{\rm N})$ is some slowly changing function of the nadir angle and $\Delta\tau_{\rm night}$ is the total duration of the night in terms of the Earth's axial rotation angle τ, namely, the length of the segment where $\Theta_{\rm N}(\tau) < \pi/2$ (the Sun is below the horizon).

Second, the duration of the night is, in turn, a function of the season ς. On the equinox, e.g., $\Delta\tau_{\rm night} = \pi$, while on the winter solstice, $\Delta\tau_{\rm night} \to \max$. However, the summer nights are

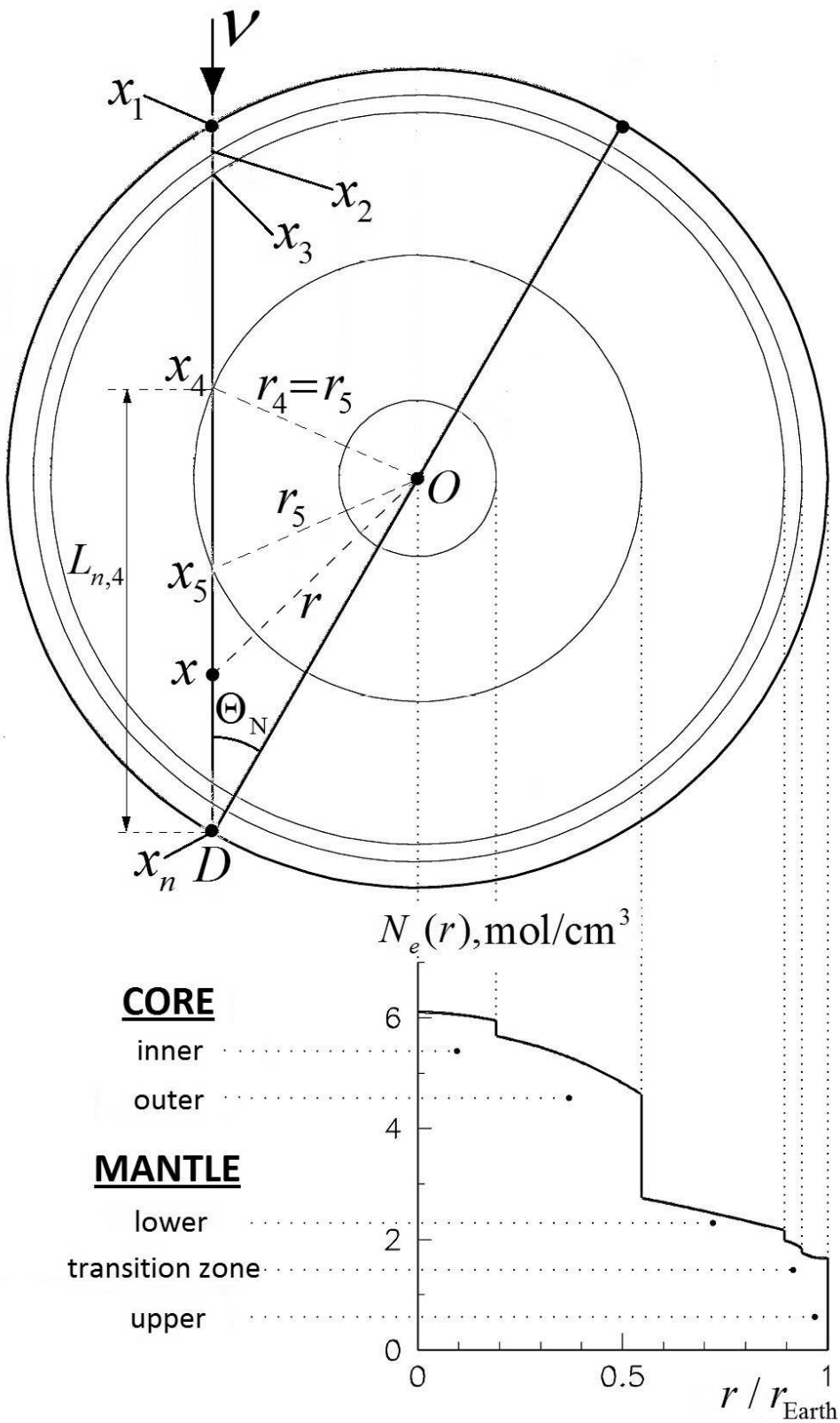

Figure 1: Radial distribution of the electron density $N_e(r)$ inside the Earth and the neutrino path through it. The figure demonstrates the cross section of the Earth which contains the nadir DO, the center of the Earth O, and the neutrino ray.

just as long as the opposite winter days, so that

$$\Delta\tau_{\rm night}(\varsigma+\pi)=2\pi-\Delta\tau_{\rm night}(\varsigma), \tag{43}$$

and the total duration of the nights over all the year is exactly half the year. Therefore, the averaging over the year of N_ς days should involve the division by the total duration of the nights, i.e., πN_ς. For $N_\varsigma\gg 1$, the summation over the nights can be replaced by the integration,

$$\langle\ldots\rangle_{\rm night,year}=\frac{1}{N_\varsigma\pi}\sum_{\varsigma=\varsigma_k}\int {\rm d}\tau(\ldots)\approx\frac{1}{2\pi^2}\int\limits_0^{2\pi}{\rm d}\varsigma\int{\rm d}\tau(\ldots),\qquad \varsigma_k=\frac{2\pi k}{N_\varsigma},k=1,\ldots,N_\varsigma, \tag{44}$$

and the averaging formula for the terms containing the phase incursion $\Delta\psi_{n,j}$ takes the form

$$\langle F(\Theta_{\rm N})e^{2{\rm i}\Delta\psi_{n,j}}\rangle_{\rm night,year}=\frac{1}{2\pi^2}\int\limits_0^{2\pi}{\rm d}\varsigma\int\limits_{\Theta_{\rm N}(\tau,\varsigma)\le\arcsin r_j/r_n}{\rm d}\tau\;F(\Theta_{\rm N}(\tau,\varsigma))\,e^{2{\rm i}\Delta\psi_{n,j}(\Theta_{\rm N}(\tau,\varsigma))}. \tag{45}$$

Now we are able to apply the stationary phase technique to such an integral containing the rapidly oscillating exponential. Indeed, let us use the expression, which is valid for smooth functions $f(x)$ and $S(x)$ defined on a segment $[a,b]$ containing a single non-degenerate stationary point $x_0\in(a,b)$ such that $S'(x_0)=0$, $S''(x_0)\ne 0$ [29]

$$\int\limits_a^b f(x)e^{{\rm i}\lambda S(x)}{\rm d}x=\sqrt{\frac{2\pi}{\lambda|S''(x_0)|}}f(x_0)\exp\left\{{\rm i}\lambda S(x_0)+{\rm i}\frac{\pi}{4}\,{\rm sgn}\,S''(x_0)\right\}+\left.\frac{f(y)e^{{\rm i}\lambda S(y)}}{{\rm i}\lambda S'(y)}\right|_a^b+O(\lambda^{-3/2}), \tag{46}$$

The two leading terms come from the stationary point and the boundary, respectively. However, in the application to the integral (42), the boundary term vanishes. Indeed, the boundary of the integration domain corresponds to the neutrino ray being tangent to the interface with radius r_j, hence, $\partial_\tau\Delta\psi_{n,j}\propto\partial_\tau L_{n,j}(\Theta_{\rm N}(\tau))\to\infty$, and the boundary term is absent. On the other hand, the stationary point is obviously achieved at midnight, when the nadir angle $\Theta_{\rm N}\to\min$ (the Sun is in its lowest position), so the integration over the night yields

$$\int\limits_{\Theta_{\rm N}(\tau)\le\arcsin r_j/r_n}F(\Theta_{\rm N}(\tau))\,e^{2{\rm i}\Delta\psi_{n,j}(\Theta_{\rm N}(\tau))}\,\frac{{\rm d}\tau}{\pi}=\left.\sqrt{\frac{1}{\pi\lambda|\partial_\tau^2L_{n,j}|}}F(\Theta_{\rm N})e^{2{\rm i}\Delta\psi_{n,j}\mp{\rm i}\pi/4}\right|_{\rm midnight}+O((\lambda L_{n,j})^{-\frac{3}{2}}), \tag{47}$$

where the two possible signs before ${\rm i}\pi/4$ correspond to $L_{n,j}=L_{n,j}^{\pm}$ (see Eq. (40)). The principal point here is that the second derivative $\partial_\tau^2L_{n,j}$ at midnight is suppressed for the inner Earth's shells,

$$\left[\partial_\tau^2L_{n,j}(\Theta_{\rm N}(\tau))\right]_{\rm midnight}=\left[\partial_\tau^2(\cos\Theta_{\rm N})\frac{{\rm d}L_{n,j}(\Theta_{\rm N})}{{\rm d}(\cos\Theta_{\rm N})}\right]_{\rm midnight}, \tag{48}$$

$$\left[\frac{{\rm d}L_{n,j}(\Theta_{\rm N})}{{\rm d}(\cos\Theta_{\rm N})}\right]_{\rm midnight}=\pm\left[\frac{L_{n,j}(\Theta_{\rm N})}{\sqrt{r_j^2/r_n^2-\sin^2\Theta_{\rm N}}}\right]_{\rm midnight}. \tag{49}$$

Now let us use the expression of the nadir angle $\Theta_{\rm N}$ via the Earth's axial tilt $\varepsilon=23.5^{\rm o}$, the latitude of the detector $\chi\in[-\pi/2,\pi/2]$, and the season $\varsigma\in[0,2\pi]$ [30],

$$\cos\Theta_{\rm N}(\tau,\varsigma)=\cos\chi\sin\varsigma\sin\tau+\cos\varepsilon\cos\chi\cos\varsigma\cos\tau+\sin\varepsilon\sin\chi\cos\varsigma, \tag{50}$$

where $\varsigma = 0$ corresponds to the winter solstice in the northern hemisphere. The midnight corresponds to the minimum value of $\Theta_{\rm N}$, which is achieved at $\tau = \tau_{\rm midnight}$,

$$\tan\tau_{\rm midnight}(\varsigma) = \frac{\tan\varsigma}{\cos\varepsilon}, \quad \cos\tau_{\rm midnight}(\varsigma) = {\rm sgn}(\cos\varsigma)\frac{\cos\varepsilon}{\sqrt{\cos^2\varepsilon+\tan^2\varsigma}}. \tag{51}$$

Using these expressions, we find the derivative of $\cos\Theta_{\rm N}$ at midnight,

$$\left[\partial_\tau^2(\cos\Theta_{\rm N})\right]_{\rm midnight} = -\frac{\cos\chi}{|\cos\varsigma|}\,\frac{\cos^2\varepsilon+\sin^2\varsigma\sin^2\varepsilon}{\sqrt{\cos^2\varepsilon+\tan^2\varsigma}} \equiv -\mathcal{N}(\varsigma), \tag{52}$$

Finally, the integral over the night (47) takes the form

$$\int\limits_{\Theta_{\rm N}(\tau)\le\arcsin r_j/r_n} F(\Theta_{\rm N}(\tau))\,e^{2{\rm i}\Delta\psi_{n,j}(\Theta_{\rm N}(\tau))}\,\frac{{\rm d}\tau}{\pi} \approx \frac{1}{\sqrt{\mathcal{N}(\varsigma)}}\left[\frac{(r_j^2/r_n^2-\sin^2\Theta_{\rm N})^{1/4}}{\sqrt{\pi\lambda L_{n,j}(\Theta_{\rm N})}}F(\Theta_{\rm N})e^{2{\rm i}\Delta\psi_{n,j}\mp{\rm i}\pi/4}\right]_{\rm midnight}. \tag{53}$$

On the other hand, the midnight stationary (minimum) values of the nadir angle $\Theta_{\rm N}(\tau_{\rm midnight})$ vary throughout the year (see Eq. (51)), being the smallest on the winter solstice (the darkest midnight) and the largest on the opposite summer solstice (the lightest midnight). Therefore, the right side of Eq. (53) is still containing a rapidly oscillating function of the season ς, and we can perform another isolation of the stationary points, namely, of the two solstices $\varsigma = 0, \pi$:

$$\langle F(\Theta_{\rm N})e^{2{\rm i}\Delta\psi_{n,j}}\rangle_{\rm night,year} = \int\limits_0^{2\pi}\frac{{\rm d}\varsigma}{2\pi}\int\limits_{\Theta_{\rm N}(\tau,\varsigma)\le\arcsin r_j/r_n} F(\Theta_{\rm N}(\tau,\varsigma))\,e^{2{\rm i}\Delta\psi_{n,j}(\Theta_{\rm N}(\tau,\varsigma))}\,\frac{{\rm d}\tau}{\pi}$$

$$= \frac{1}{2\pi}\sum_{\varsigma=0,\pi}\frac{1}{\sqrt{\mathcal{N}(\varsigma)|\partial_\varsigma^2\cos\Theta_{\rm N}(\tau_{\rm midnight}(\varsigma))|}}\left[\frac{\sqrt{r_j^2/r_n^2-\sin^2\Theta_{\rm N}}}{\lambda L_{n,j}(\Theta_{\rm N})}F(\Theta_{\rm N})e^{2{\rm i}\Delta\psi_{n,j}\pm{\rm i}(s-1)\pi/4}\right]_{\rm midnight}, \tag{54}$$

$$\partial_\varsigma^2\cos\Theta_{\rm N}(\tau_{\rm midnight}(\varsigma)) = \begin{cases}\sin(\varepsilon-\chi)\tan\varepsilon, & \varsigma=0 \text{ (winter solstice)},\\ \sin(\varepsilon+\chi)\tan\varepsilon, & \varsigma=\pi \text{ (summer solstice)},\end{cases} \tag{55}$$

$$s \equiv {\rm sgn}\left\{\partial_\varsigma^2\cos\Theta_{\rm N}(\tau_{\rm midnight}(\varsigma))\right\} = \begin{cases}-1, & \varsigma=0,\\ +1, & \varsigma=\pi.\end{cases} \tag{56}$$

The signs specified in the latter expression are valid in the northern non-tropical latitudes $\chi > \varepsilon$. The detector used by the Borexino collaboration is situated in the Gran Sasso laboratory, with $\theta = +42.5^{\rm o}$, and the prefactor in (54) which does not depend on j amounts to be

$$\frac{1}{2\pi\sqrt{\mathcal{N}(\varsigma)|\partial_\varsigma^2\cos\Theta_{\rm N}(\tau_{\rm midnight}(\varsigma))|}} = \frac{1}{2\pi\sqrt{\sin\varepsilon\cos\chi|\sin(\varepsilon\mp\chi)|}} \approx \begin{cases}0.51, & \text{winter solstice},\\ 0.31, & \text{summer solstice}.\end{cases} \tag{57}$$

Therefore, we are left with the following conclusion. The terms entering Eq. (39), which contain the oscillating functions of the phase incursions $2\Delta\psi_{n,j}$, are suppressed as $O\left(\frac{r_j}{r_n\lambda L_{n,j}}\right) = O\left(\frac{r_j}{r_n}\delta\right)$ after averaging over the year; within the leading approximation, the resulting averages (54) come from the stationary phase points achieved on the winter and the summer solstices. The suppression becomes stronger for the inner Earth's shells.

It is spectacular that all the terms of the order $O(\eta\delta)$ in the expression (39), including the one corresponding to the detector, become $O(\eta\delta^2 r_j/r_n)$ after the averaging. The terms of the order $O(\eta)$, which are proportional to $\Delta\theta_j$, become $O(\eta\delta r_j/r_n)$, respectively. Finally, we are left with the average value

$$\langle T_{\rm night}\rangle = \cos 2\theta_{\rm Sun}\cos 2\theta_n^- + O\left(n\eta\delta\frac{r_j}{r_n}\right). \tag{58}$$

By substituting this result together with the daytime average value (33) into expression (27) for the neutrino observation probabilities, we arrive at the day-night asymmetry factor

$$A_{\rm dn} \equiv \frac{2(\langle P_{e,\rm night}\rangle - \langle P_{e,\rm day}\rangle)}{\langle P_{e,\rm night}\rangle + \langle P_{e,\rm day}\rangle} = -\frac{T_{\rm MSW}}{1+T_{\rm MSW}} \cdot \frac{\sin^2 2\theta_0}{\cos 2\theta_0} \frac{2EV(x_n^-)}{\Delta m^2} + O\left(n\eta\delta \frac{r_j}{r_n}\right), \qquad (59)$$

where $T_{\rm MSW} = \cos 2\theta_0 \cos 2\theta_{\rm Sun} = a_{\rm vac} a_{\rm Sun}/\omega_{\rm Sun}$ defines the observation probabilities for the solar neutrinos due to the Mikheev–Smirnov–Wolfenstein effect [2] and $V(x_n^-)$ is the Wolfenstein potential in the Earth's crust under the detector.

3.3 The effect of the crust

The estimation (59) shown above is substantially based on the piecewise continuous structure of the density profile and shows that the asymmetry should depend only on the density of rock immediately under the detector, i.e. in the Earth's crust. At the same time, the actual width of the crust is comparable with the oscillation length, and neither the valley nor the cliff approximation is valid for this layer. Moreover, the phase incursions are small within the crust, and so do their time variations, hence, we are unable to use the stationary phase approximation. However, we are still able to account for the effect of the crust on the observed day-night asymmetry factor (59), relying upon its relatively small density. This feature, together with its bounded thickness, makes it possible to find the closed form of the approximate flavor evolution operator for the crust $[x_{n-1}^+, x_n^-]$:

$$R_0(x_n^-, x_{n-1}^+) = \exp\{(-{\rm i}\sigma_2\beta + {\rm i}\sigma_1\alpha) e^{2{\rm i}\sigma_3\psi(x_{n-1}^+)}\} + O(\eta^2), \qquad (60)$$

$$\beta + {\rm i}\alpha = \int\limits_{x_{n-1}^+}^{x_n^-} \dot\theta(y) e^{2{\rm i}(\psi(y) - \psi(x_{n-1}^+))} {\rm d}y, \qquad \alpha, \beta = O(\eta) \in \mathbb{R}. \qquad (61)$$

This result formally repeats the cliff approximation (19) up to the substitution $\Delta\theta_j \to \beta$, $\mu_j \to \alpha$. Then, exactly the same modification arises in (39),

$$\begin{aligned} T_{\rm night} = \cos 2\theta_{\rm Sun} \Big\{ & \cos 2\theta_n^- + 2\sin 2\theta_n^- \textstyle\sum_{j=1}^{n-1} (\Delta\theta_j \cos 2\Delta\psi_{n,j} + \bar\mu_j \sin 2\Delta\psi_{n,j}) \\ & -4\Delta\psi_{\rm det} \sin 2\theta_{\rm det} \textstyle\sum_{j=1}^{n-1} \Delta\theta_j \sin 2\Delta\psi_{n,j} \Big\} + \Delta T_{\rm night}, \end{aligned} \qquad (62)$$

$$\begin{aligned} \Delta T_{\rm night} &= \cos 2\theta_{\rm Sun} \{ 2\sin 2\theta_n^- (\beta \cos 2\Delta\psi_{n,n-1} + \alpha \sin 2\Delta\psi_{n,n-1}) \\ &\quad -4\Delta\psi_{\rm det} \sin 2\theta_{\rm det} (\beta \sin 2\Delta\psi_{n,n-1} - \alpha \cos 2\Delta\psi_{n,n-1}) \} \\ &= 2\cos 2\theta_{\rm Sun} \sin 2\theta_n^- \int\limits_{x_{n-1}^+}^{x_n^-} \dot\theta(y) \cos 2\Delta\psi(y)\, {\rm d}y \\ &\quad -4\cos 2\theta_{\rm Sun} \Delta\psi_{\rm det} \sin 2\theta_{\rm det} \int\limits_{x_{n-1}^+}^{x_n^-} \dot\theta(y) \sin 2\Delta\psi(y)\, {\rm d}y, \end{aligned} \qquad (63)$$

where $\Delta\psi(y) \equiv \psi(x_n^-) - \psi(y)$. The leading $O(\eta)$ correction of the crust to the day-night asymmetry factor (59) reads

$$\Delta A_{\rm dn} = \frac{T_{\rm MSW}}{1+T_{\rm MSW}} \cdot \frac{\sin^2 2\theta_0}{\cos 2\theta_0} \frac{2E}{\Delta m^2} \int\limits_{x_{n-1}^+}^{x_n^-} \dot V(y) \cos 2\Delta\psi(y)\, {\rm d}y. \qquad (64)$$

Again, this result should be subjected to the averaging procedure to acquire the predictive power. However, due to the boundedness of the cosine, the correction is easily estimated (both before and after averaging),

$$\left|\frac{(\Delta A_{\rm dn})}{A_{\rm dn}}\right| \le \frac{1}{V(x_n^-)} \int\limits_{x_{n-1}^+}^{x_n^-} |\dot{V}(y)| {\rm d}y \sim \frac{|(\Delta V)_{\rm crust}|}{V(x_n^-)}. \qquad (65)$$

Within the Earth's crust, the density change is within 20–30%, hence the change of the Wolfenstein potential $|(\Delta V)_{\rm crust}| \le 0.25 V(x_n^-)$. Thus, the non-trivial structure of the crust could produce the deviation of the day-night asymmetry factor from expression (59) only within 20–30%. The only exception from this rule may occur if the detector is placed above the deep region of the ocean (here, both the crust-to-ocean and ocean-to-air jumps of the potential are quite large). In this case, the day-night asymmetry factor can be readily found using Eq. (64) and may become substantially smaller than the one measured by the continental detector.

4 Discussion

From expressions (59) and (64), one can see that the asymmetry has the order $O(\eta)$ and is determined by the rock density in the layer under the detector, i.e. in the Earth's crust. Using the recent data from the SNO and KamLAND collaborations [7, 8], namely, $\tan^2\theta_0 \approx 0.46$ and $\Delta m^2 \approx 7.6 \times 10^{-5}$ eV^2, and the typical electron densities in the Earth's crust $N_{e({\rm crust})} = 1.3\,{\rm mol/cm^3}$ [27] and in the solar core $N_{e({\rm Sun})} \sim 100$ mol/cm^3 [31], we arrive at the numerical estimation for the day-night asymmetry factor for solar beryllium-7 neutrinos ($E = 0.862\,{\rm MeV}$)

$$A_{\rm dn} = (-3.8 \pm 0.9) \times 10^{-4}. \qquad (66)$$

The uncertainty corresponds to the effect of the Earth's crust, which, in principle, can be explicitly evaluated by numerical averaging of Eq. (64). Formally, our estimation is in agreement with the results of the Borexino experiment on the day-night asymmetry [6],

$$A_{\rm dn}^{\rm (Borexino)} = \big(1 \pm 12({\rm stat.}) \pm 7({\rm syst.})\big) \times 10^{-3}. \qquad (67)$$

The leading corrections not shown in (66) come from the averaging over the oscillation phases inside the Earth and are suppressed as $O\left(\frac{r_j}{r_n}\frac{\ell_{\rm osc}}{L_{n,j}}\right)$. This suppression is quite strong for dense though deep inner Earth's shells, including its core. For the typical number of the valleys $n \sim 10$, the total contribution of these corrections is several times smaller than the effect of the crust specified in (66).

The energy dependence of the predicted day-night asymmetry factor (59) within the domain $E < 3\,{\rm MeV}$ is shown in Fig. 2. We observe that the asymmetry vanishes for the low-energy neutrinos, which is a result of the applicability of the adiabatic approximation for such neutrinos. Indeed, within this approximation, the neutrino flavor observation probabilities depend only on the creation and absorbtion points.

For the neutrinos with energies $E \gtrsim 3\,{\rm MeV}$, Eq. (59) becomes only qualitative. For instance, the energies of the boron neutrinos, which were considered, e.g., in the paper [25], reach 10 MeV, while the oscillation lengths are as large as 300 km. For such energies, both the relative errors of the valley solutions (18) (multiplied by their number $n \sim 10$) and the averaging errors may, in principle, become quite large.

One should also mention here that, although the day-night asymmetry factor is a quantity which is directly measured in the neutrino experiments, both its sign and magnitude depend not only on the neutrino regeneration effect inside the Earth, but also on the value of the Wolfenstein potential in the solar core, where the neutrino is created. This fact is easily seen

in (59), where the solar effect manifests itself via the quantity $T_{\rm MSW}$, which depends on the neutrino energy E. At the energy $E \sim 2.3\,{\rm MeV}$, which corresponds to the Mikheev–Smirnov resonance, we have $a_{\rm Sun} = 0$ and $T_{\rm MSW} = 0$, and, as a consequence, the day-night asymmetry factor (59) changes sign (see Fig. 2). Thus, it is the resonance inside the Sun which makes the asymmetry, observed on the Earth, vanish.

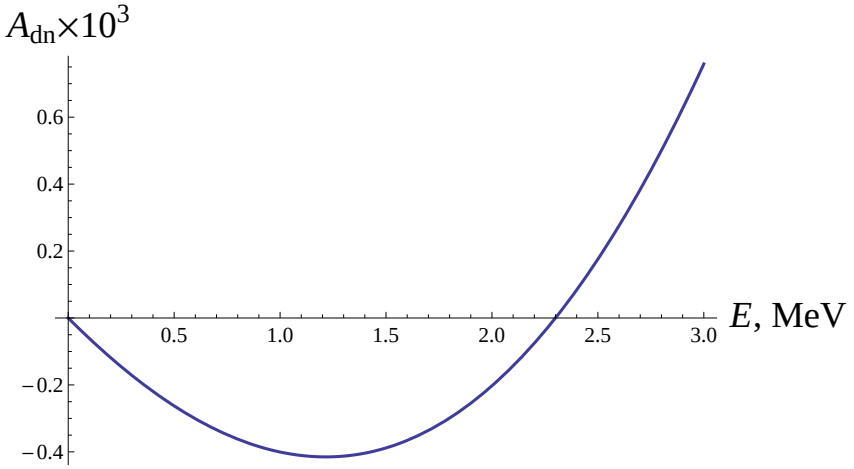

Figure 2: The predicted day-night asymmetry factor $A_{\rm dn}$ as a function of the neutrino energy E plotted for $\Delta m^2 = 7.6 \times 10^{-5}{\rm eV}^2$ and $\tan^2\theta_0 = 0.46$.

Finally, one may observe that beryllium neutrinos ($E = 0.862\,{\rm MeV}$) are indeed quite useful for the study of the matter effects in the neutrino oscillations, since they correspond to almost maximum negative asymmetry factor. Moreover, solar beryllium neutrinos are highly monochromatic (in contrast, e.g., to the boron neutrinos) and their flux is considerably larger [31]. Thus the Borexino experiment is a prospective attempt to detect the day-night flavor asymmetry. However, we are able to conclude that the latter effect needs a 10–20 times better experimental resolution to be distinguished at a considerable confidence level. This conclusion does not depend on the densities of the inner Earth's layers and on the substance and the dimensions of the detector, as far as they are considerably smaller than the oscillation length.

As a demonstration of our conclusions about the time average of the day-night asymmetry factor, we present the results of its numerical averaging, together with the theoretical curve (59), in Fig. 3. The two dotted curves correspond to the neutrino detectors placed in Gran Sasso ($\chi = +42.5^{\rm o}$) and on the Northern tropic ($\chi = +\varepsilon = +23.5^{\rm o}$). The latter curve demonstrates specific oscillations which come from the amplified contribution of the winter solstice stationary point to the year average of the asymmetry factor (see Eq. (54)). Moreover, the approximate smoothness of the both curves indicates the (approximate) stability of the day-night asymmetry factor with respect to slight variations of the parameters of the PREM model, namely, the radii of the Earth's shells and the density jumps. The stability becomes stronger for low-energy neutrinos, as well as for the detectors operating far from the tropic.

It is also interesting to study the effect of the local Earth's crust inhomogeneities under the detector on the observed day-night asymmetry. Such inhomogeneities could be associated, for instance, with the oil-bearing horizons. Let the inhomogeneity be described by the variation $\delta N_e^{\rm (i)}(x)$ of the electron density over the smooth profile $\bar{N}_e(x)$,

$$N_e(x) = \bar{N}_e(x) + \delta N_e^{\rm (i)}(x), \qquad \delta N_e^{\rm (i)}(x) = 0 \text{ for } x \notin [x_{\rm i}, x_{\rm i} + \delta x_{\rm i}], \tag{68}$$

where the inhomogeneity size $\delta x_{\rm i} \ll \ell_{\rm osc}$. Then the contribution of this inhomogeneity to the

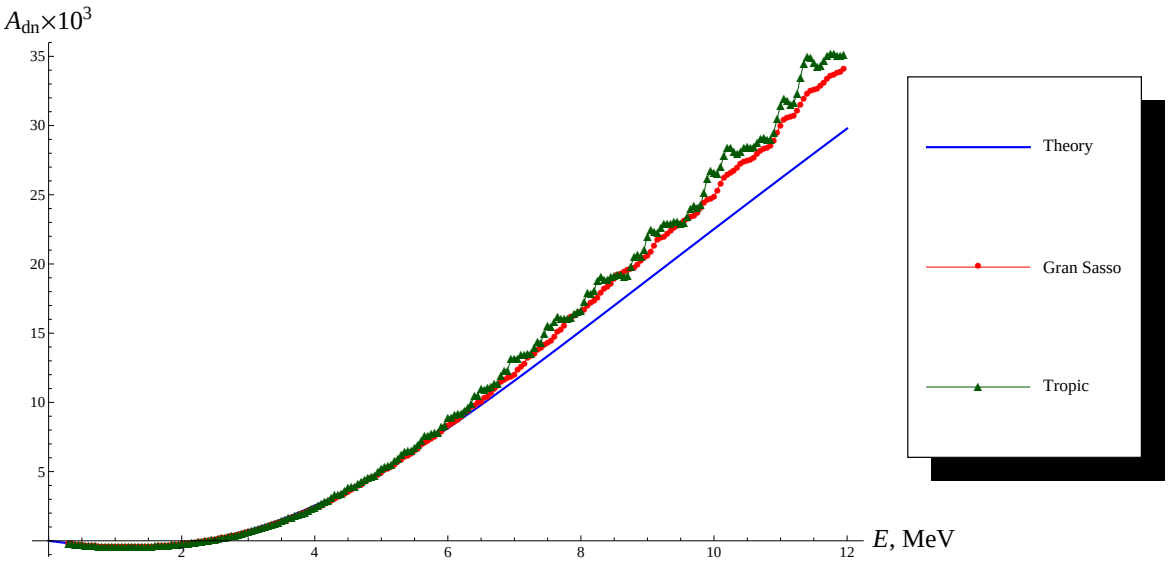

Figure 3: Numerically averaged day-night asymmetry factor versus the predicted one for different neutrino energies E. The curves with circle and triangle fit points correspond to the neutrino detectors placed in Gran Sasso ($\chi = +42.5^{\rm o}$) and on the Northern tropic ($\chi = +\varepsilon = +23.5^{\rm o}$), respectively. The solid curve corresponds to the theoretical estimation (59) of the average asymmetry.

asymmetry factor is given by Eq. (64),

$$\begin{aligned}\frac{\delta A_{\rm dn}^{\rm (i)}}{A_{\rm dn}} &= -\frac{1}{N_{e({\rm crust})}} \int\limits_{x_{\rm i}}^{x_{\rm i}+\delta x_{\rm i}} \delta\dot{N}_e^{\rm (i)}(y)\cos 2\Delta\psi(y){\rm d}y \\ &= \frac{1}{N_{e({\rm crust})}} \int\limits_{x_{\rm i}}^{x_{\rm i}+\delta x_{\rm i}} \delta N_e^{\rm (i)}(y)\sin 2\Delta\psi(y)\frac{2\pi\omega(y){\rm d}y}{\ell_{\rm osc}},\end{aligned} \tag{69}$$

$$\left|\frac{\delta A_{\rm dn}^{\rm (i)}}{A_{\rm dn}}\right| \le \frac{|\delta N_e^{\rm (i)}|}{N_{e({\rm crust})}}\frac{2\pi\delta x_{\rm i}}{\ell_{\rm osc}}\left|\sin\frac{2\pi L^{\rm (i)}}{\ell_{\rm osc}}\right|, \tag{70}$$

where $L^{\rm (i)} = x_n^- - x_{\rm i}$ is the depth of the inhomogeneity under the detector. Therefore, exploration of the Earth's crust based on the neutrino oscillations would require an extreme improvement of current measurement techniques [32], and its prospects seem obscure in the nearest future.

Acknowledgments

The authors are grateful to A. V. Borisov and V. Ch. Zhukovsky for fruitful discussions of the ideas of the present paper. The authors would also like to thank Wei Liao for his stimulating remarks concerning the averaging procedure. Finally, we should thank E. Lisi and D. Montanino for Fig. 1 in their paper [21], which we have used for creating Fig. 1 in the present manuscript.

References

[1] L. Wolfenstein, Phys. Rev. D **17**, 2369 (1978).

[2] S. Mikheev and A. Smirnov, Yad. Fiz. **42**, 1441 (1985) [Sov. J. Nucl. Phys. **42**, 913 (1985)].

[3] H. A. Bethe, Phys. Rev. Lett. **56**, 1305 (1986).

[4] E. D. Carlson, Phys. Rev. D **34**, 1454 (1986).

[5] A. J. Baltz and J. Weneser, Phys. Rev. D **35**, 528 (1987).

[6] G. Bellini *et al.*, Phys. Lett. B **707**, 22 (2012).

[7] B. Aharmim *et al.*, Phys. Rev. Lett. **101**, 111301 (2008).

[8] S. Abe *et al.*, Phys. Rev. Lett. **100**, 221803 (2008).

[9] V. Bargmann, L. Michel, and V. Telegdi, Phys. Rev. Lett. **2**, 435 (1959).

[10] A. E. Lobanov and O. S. Pavlova, Teoret. Mat. Fiz. **121**, 509 (1999) [Theor. Math. Phys. **121**, 1691 (1999)].

[11] E. A. Coddington and N. Levinson, *Theory of Ordinary Differential Equations* (McGraw-Hill, New York, 1955).

[12] A. E. Lobanov, Vestn. MGU. Fiz. Astron. **38**, No. 2, 59 (1997) [Moscow Univ. Phys. Bull. **52**, No. 2, 85 (1997)].

[13] V. G. Bagrov, D. M. Gitman, M. C. Baldiotti, and A. D. Levin, Annalen der Physik **14**, 764 (2005).

[14] W. Magnus, Commun. Pure Appl. Math. **7**, 649 (1954).

[15] J. E. Campbell, Proc. London Math. Soc. **28**, 381 (1897).

[16] S. Blanes, F. Casas, J. A. Oteo, and J. Ros, Phys. Rept. **470**, 151 (2009).

[17] J. C. D'Olivo and J. A. Oteo, Phys. Rev. D **42**, 256 (1990).

[18] J. C. D'Olivo, Phys. Rev. D **45**, 924 (1992).

[19] A. D. Supanitsky, J. C. D'Olivo, and G. A. Medina-Tanco, Phys. Rev. D **78**, 045024 (2008).

[20] A. N. Ioannisian and A. Yu. Smirnov, Nucl. Phys. B **816**, 94 (2009).

[21] E. Lisi and D. Montanino, Phys. Rev. D **56**, 1792 (1997).

[22] M. Blennow and T. Ohlsson, J. Math. Phys. **45**, 4053 (2004).

[23] E. Kh. Akhmedov and V. Niro, JHEP **12(2008)**, 106 (2008).

[24] A. N. Ioannisian and A. Yu. Smirnov, Phys. Rev. Lett. **93**, 241801 (2004).

[25] P. C. de Holanda, Wei Liao, and A. Yu. Smirnov, Nucl. Phys. B **702**, 307 (2004).

[26] A. M. Dziewonski and D. L. Anderson, Phys. Earth Planet. Inter. **25**, 297 (1981).

[27] D. L. Anderson, *Theory of the Earth* (Blackwell Scientific Publications, Boston, 1989).

[28] A. N. Ioannisian, N. A. Kazarian, A. Yu. Smirnov, and D. Wyler, Phys. Rev. D **71**, 033006 (2005).

[29] M. V. Fedoruk, *The Method of Steepest Descent* (Nauka, Moscow, 1977) [in Russian].

[30] R. M. Green, *Spherical Astronomy* (Cambridge University Press, Cambridge, UK, 1985).

[31] J. Bahcall, *Neutrino astrophysics* (Cambridge University Press, Cambridge, UK, 1989).

[32] A. N. Ioannisian and A. Yu. Smirnov, e-Print arXiv:hep-ph/0201012.